Phase equilibria of asymmetric hard sphere mixtures

N. G. Almarza and E. Enciso
Departamento de Química Física I, Facultad de Ciencias Químicas, Universidad Complutense, E-28040 Madrid, Spain
(Received 4 September 1998; revised manuscript received 3 December 1998)

The phase diagram of mixtures of hard spheres with additive diameters is studied. The case of very different sizes is treated by means of mapping the two component system on a one component problem. In this monocomponent system large particles are explicitly considered, whereas the effects of the small component are included through an additional effective interaction potential between large particles. The effective potential is used to analyze the phase diagram of the mixture by means of computer simulation techniques. Results for the behavior at low density of small spheres seem to indicate that no fluid-fluid equlibria occur. On the other hand, the results show how this kind of mixture can exhibit equilibria between isostructural crystalline phases. [S1063-651X(99)08204-5]

PACS number(s): 05.20.−y, 64.75.+g, 82.70.Dd

I. INTRODUCTION

The phase equilibria of asymmetric hard sphere mixtures (AHSM) has become a problem which has received a lot of attention in recent years [1]. The existence of fluid-fluid equilibria in AHSM has been predicted from theoretical approaches; however, the results of different approximate theories are very discrepant [1]. Standard computer simulation methods are not very effective when applied to these systems: the interesting results are supposed to appear at high packing fractions of both components when the particle sizes are quite different, this leads us to consider systems with a high number of particles of small species in order to have a sensible number of large particles, furthermore, the systems suffer from a serious additional problem: the diffusion of large particles is quite hindered by the presence of many small particles which makes equilibration an impossible task. One of the most popular methods to simulate fluid-fluid equilibria, the so called Gibbs ensemble Monte Carlo method [2], is not useful in this context. In this case the problem is due to the difficulties in designing effective methods to insert large particles in the system.

It is known that in a system composed of a solute of large particles and a solvent of small particles the difference in size can induce some attraction between large particles [3,4], due to excluded volume effects which produce the so called depletion forces. These effects are supposed to be short ranged in the large particle size scale. Some effort has been devoted to parametrizing the form of these induced interactions between solute particles [5–10]. The influence of such effects on the phase equilibria of the system is the main point in this work. On the other hand, in recent years some attention has been devoted to evaluating the effect of the potential range in the phase diagram of simple fluids. One of the most interesting findings is that, for systems interacting through a hard core potential plus a very short ranged attractive interaction, the liquid does not appear as stable phase [11,12]. In addition, for very short range potentials, equilibria between two crystalline phases with the same symmetry have been found [13]. Such equilibria end for high temperatures at a critical point. One question that arises after watching these facts is whether the phase diagram of very asymmetric hard sphere mixtures could show this kind of phenomenology. Preliminary results [14] seem to indicate such a behavior. In this work we explore a combination of different methods of statistical mechanics to determine the phase diagram of these systems. The procedure lies in the possibility of mapping the two component system in a one component system with an effective pair potential which depends on the activity of the solvent. This mapping procedure is based on the theoretical framework of the statistical mechanics of simple fluids in external fields. The use of an effective potential of a monocomponent system allows us to use a number of simulation techniques to explore the phase diagram without needing to use a very large number of particles or very long runs.

The paper is sketched as follows. In Sec. II we show an accurate route to map the two component system in a one component problem. Section III is devoted to the procedures used to determine the phase diagram. In Sec. IV we mention the main simulation details. In Sec. V the main results are shown, including the phase diagram and some tests to check the ability of the effective potential formalism to reproduce the results of the binary system. Finally, in Sec. VI the main conclusions are collected.

II. STATISTICAL MECHANICS

We will deal with binary mixtures of hard spheres. The hard sphere (HS) diameters will be σ_s and σ_l ($\sigma_l > \sigma_s$). The size ratio is defined as $R = \sigma_s / \sigma_l$. Components s and l will be referred to as the solvent and solute, respectively. The aim of this work is to solve the statistical problem of the mixtures by considering a fluid of solute particles interacting through some effective potential which will depend on the chemical potential (or other related property) of the solvent.

The partition function Q in an ensemble defined by $\beta = 1/(k_B T)$, βp, z_s, and N_l, where k_B is the Boltzmann constant, T is the absolute temperature, p is the pressure, and $z_s \propto e^{\beta \mu_s}$ is the activity of the solvent (with μ_s being the chemical potential of the solvent) reads

$$Q = \frac{1}{\Lambda_l^{3N_l} N_l!} \int dV\, V^{N_l} e^{-\beta p V} \int d\mathbf{q}_l e^{-\beta U_{LL}(\mathbf{q}_l, V)} e^{-\beta \Omega(z_s, V, \mathbf{q}_l)}, \tag{2.1}$$

where Λ_l is the *de Broglie* wavelength of large particles, U_{LL} represents the hard sphere interaction between solute spheres, $\mathbf{q}_l$ are the position coordinates of solute particles reduced with the system size [15], and Ω is the grand potential of the small particles for a given large particle configuration. Ω can be expanded in a series of the solvent activity considering large spheres as an external field [16].

A. First-order expansion

The expansion of Ω up to first order produces

$$-\beta\Omega^{(1)}=z_s I_1(V,\mathbf{q}_l), \tag{2.2}$$

where I_1 is the volume available for small spheres. I_1 is a function of the position coordinates of the large particles. Positions lying at a distance less than $\sigma_{sl}=(\sigma_s+\sigma_l)/2$ of a solute particle are not accessible to solvent particles. I_1 can be written as

$$I_1=V-\sum_i w_i+\sum_{i<j} w_{ij}-\sum_{i<j<k} w_{ijk}+\cdots, \tag{2.3}$$

where w_i represents the amount of volume excluded to the solvent by the ith particle, and w_{ij} is the overlap between the volumes excluded to the solvent by particles i and j, etc. The hard sphere interaction between solute particles makes the truncation of the series possible. The number of terms to consider depends on the size ratio. From simple geometric considerations [17] it follows that for values of $R\leqslant 2/\sqrt{3}-1\equiv R_2\simeq 0.1547$, the hard sphere interaction between large spheres avoid the existence of an intersection of the volumes excluded by three large spheres. Therefore, for $R\leqslant R_2$,

$$I_1=V-N_l v_l\alpha^3+\sum_{i<j} S(\sigma_{sl},r_{ij}), \tag{2.4}$$

where $v_l=\pi\sigma_l^3/6$ is the solute particle volume, $\alpha\equiv 1+R=(2\sigma_{sl})/\sigma_l$, and $S(\sigma,r)$ is the overlapping volume between two spheres of radius σ at distance r. Using the definition of α, such a volume can be written as

$$S(\sigma_{sl},r)=\frac{\pi\sigma_l^3}{12}\left(\alpha-\frac{r}{\sigma_l}\right)^2\left(2\alpha+\frac{r}{\sigma_l}\right) \tag{2.5}$$

for $r/\sigma_l\leqslant\alpha$, and 0 otherwise. The partition function of the system in the limit of low activities of the small component is

$$Q^{(1)}=\frac{1}{\Lambda_l^{3N_l}N_l!}\int dV\,V^{N_l}e^{-\beta pV+z_sV-z_sN_lv_l\alpha^3}\int d\mathbf{q}_l\exp\left[\sum_{ij}\left(-\beta u^{\mathrm{HS}}(r_{ij})+z_sS(\sigma_{sl},r_{ij})\right)\right], \tag{2.6}$$

where u^{HS} represents the hard sphere pair potential between solute particles, and the terms z_sS play the role of additional effective pair interactions between large spheres due to the presence of small particles. The z_s expansion of Ω up to first order does not take into account interactions between small spheres (due to the small reduced density). Considering a pure system of small spheres at the same level of approximation (first order in activity), which is at chemical equilibrium with the solvent in the mixture, it is possible to relate the activity with the density ρ_0 and pressure p_0 of such a reference system:

$$\beta p_0^{(1)}=\rho_0^{(1)}=z_s. \tag{2.7}$$

An *ad hoc* osmotic pressure $\Pi^{(1)}$ can be defined as

$$\beta\Pi^{(1)}=\beta p-z_s. \tag{2.8}$$

Introducing this definition in Eq. (2.6), we obtain

$$Q^{(1)}=\frac{\exp[-z_sN_lv_l\alpha^3]}{\Lambda_l^{3N_l}N_l!}\int dV\,V^{N_l}e^{-\beta\Pi^{(1)}V}\int d\mathbf{q}_l\exp\left[\sum_{ij}\left(-\beta u^{\mathrm{HS}}(r_{ij})+z_sS(\sigma_{sl},r_{ij})\right)\right]. \tag{2.9}$$

B. Second order

The second-order expansion of the grand potential, $\beta\Omega^{(2)}$, in terms of the activity reads

$$-\beta\Omega^{(2)}=-\beta\Omega^{(1)}+z_s^2I_2 \tag{2.10}$$

where I_2 [16] is

$$I_2(V,\mathbf{q}_l)=\tfrac{1}{2}\int d\mathbf{r}_1\exp[-\beta U_{\mathrm{LS}}(\mathbf{r_1}|V,\mathbf{q}_l)]\int d\mathbf{r}_2\exp[-\beta U_{\mathrm{LS}}(\mathbf{r_2}|V,\mathbf{q}_l)]f(r_{12}), \tag{2.11}$$

where the integration is performed over two solvent particles. f is the Mayer function of the interaction between solvent particles, and U_{LS} takes into account the hard sphere interaction between large particles with a small one. This contribution can also raise an additional pair-additive effective interaction between large spheres for small values of R ($R \leqslant R_2^{(2)} \approx 0.095$) [17]. This is not the case for $R=0.10$, one of values used in this work. A number of routes can be taken at this point in order to avoid the cumbersome task of introducing many-body contributions, One can neglect the many-body contributions, which are only relevant when three particles become very close, and evaluate the second-order contribution to the effective potential between pairs of particles [16], or consider the results in the limit of $R \to 0$ [5]. Then one can find some difficulties in the results, either because one has to parametrize numerical results for some cluster integrals in the evaluation of the pair contributions to I_2 or due to the complexity of some analytical results [5] which make them not very amenable to carrying out simulations. We have chosen to follow a different point of view, which makes simulation easier while keeping the relevant features of the system. I_2 can be regarded as the configuration integral of a diatomic molecule with a bond distance that is free to change between 0 and σ_s in a medium of large spheres. This configuration integral can be written as the product of an ideal internal part by a translational part which incorporates the interaction with the external field. This second contribution can be approximated by considering an *equivalent* sphere with an effective diameter σ_d. In this work the value of σ_d has been chosen to obtain the correct value of I_2 in the limit of high dilution of large spheres. With this criteria, the second-order contribution to the partition function can also be written in terms of pair interactions for the value $R=0.10$,

$$I_2 \simeq -B\left[V - N_l v_l \alpha_d^3 + \sum_{i<j} S(\sigma_{ld}, r_{ij})\right], \tag{2.12}$$

where $B = 2\pi\sigma_s^3/3$ is the second virial coefficient of a pure solvent system, $\sigma_{ld} = (\sigma_l + \sigma_d)/2$, $\alpha_d = 2\sigma_{ld}/\sigma_l$ and σ_{ld} can be calculated as

$$\sigma_{ld}^3 = \sigma_{ls}^3\left[1 + \frac{9R}{8(1+R)} - \frac{R^3}{4(1+R)^3}\right]. \tag{2.13}$$

Following the same procedure as in first order, the expansion of the pressure of the reference system up to second order reads

$$\beta p_0^{(2)} = z - Bz^2. \tag{2.14}$$

Therefore, introducing the *ad hoc* osmotic pressure $\beta\Pi^{(2)} = \beta p - \beta p_0^{(2)}$, we obtain the second order approach to the partition function:

$$Q^{(2)} = \frac{\exp[-N_l v_l (z_s \alpha^3 - z_s^2 B \alpha_d^3)]}{\Lambda_1^{3N_l} N_l!} \int dV\, V^{N_l} e^{-\beta\Pi^{(2)} V} \times \int d\mathbf{q}_2 e^{-\beta U_{\mathrm{effec}}^{(2)}} \tag{2.15}$$

where

$$\beta U_{\mathrm{effec}}^{(2)} = \sum_{i<j} \left[\beta u_{ij}^{\mathrm{HS}} - z_s S(\sigma_{sl}, r_{ij}) + z_s^2 B S(\sigma_{ld}, r_{ij})\right]. \tag{2.16}$$

The corresponding expressions for the expansion up to first order are recovered by setting $B=0$.

A new transformation is convenient in order to achieve better convergence behavior. That transformation consists of developing the effective potential using the density of the reference system ρ_0 instead of its activity. This is done by writing the activity as a series of the homogenous system density, substituting in Eq. (2.15), and retaining terms up to second order in ρ_0. The result is

$$z = \rho + 2B\rho^2 + \cdots, \tag{2.17}$$

$$Q_{\rho_0}^{(2)} = \frac{\exp[-N_l v_l \alpha^3 (\rho_0 + B\rho_0^2) + N_l v_l \rho_0^2 B(\alpha_d^3 - \alpha^3)]}{\Lambda_1^{3N_l} N_l!} \times \int dV\, V^{N_l} e^{-\beta\Pi^{(2)} V} \int d\mathbf{q}_2 e^{-\beta U_{\mathrm{effec}}^{(2)}}, \tag{2.18}$$

where

$$\beta\Pi^{(2)} = \beta p - (\rho_0 + B\rho_0^2), \tag{2.19}$$

$$\beta U_{\mathrm{effec}}^{(2)} = \sum_{i<j} \beta u_{effec}^{(2)}(r_{ij}) = \sum_{i<j} \left[\beta u^{HS}(r_{ij}) - \rho_0 \nu_1(r_{ij}) - B\rho_0^2 \nu_2(r_{ij})\right], \tag{2.20}$$

where

$$\nu_1(r) = S(\sigma_{sl}, r), \tag{2.21}$$

$$\nu_2(r) = 2S(\sigma_{sl}, r) - S(\sigma_{ld}, r). \tag{2.22}$$

Again, the expression for the first-order approach in terms of ρ_0 is recovered by taking $B=0$.

In Fig. 1 we compare the first- $[\nu_1(r)]$ and second-order $[\nu_2(r)]$, contributions to the effective pair potential between large spheres used in this work with those reported in Ref. [5], and the exact ones evaluated by diagrammatic expansions up to second order of the pair distribution function [16] of two large particles in a medium of small particles.

In Fig. 2 we show the realizations of the effective contributions into the total pair interaction, $\beta u_{\mathrm{effec}}^{(n)}$, for $R=0.10$ and $\rho_0\sigma_s^3 = 0.30$. In addition we plot the effective interaction using the third-order exact potential for this case, evaluated numerically by means of a diagrammatic expansion, and the result for the potential developed in Ref. [10], which also contains terms depending on ρ_0^3. This last effective interaction was used in Ref. [18] in their study of the phase diagram of AHSM using a similar approach to that employed in this work.

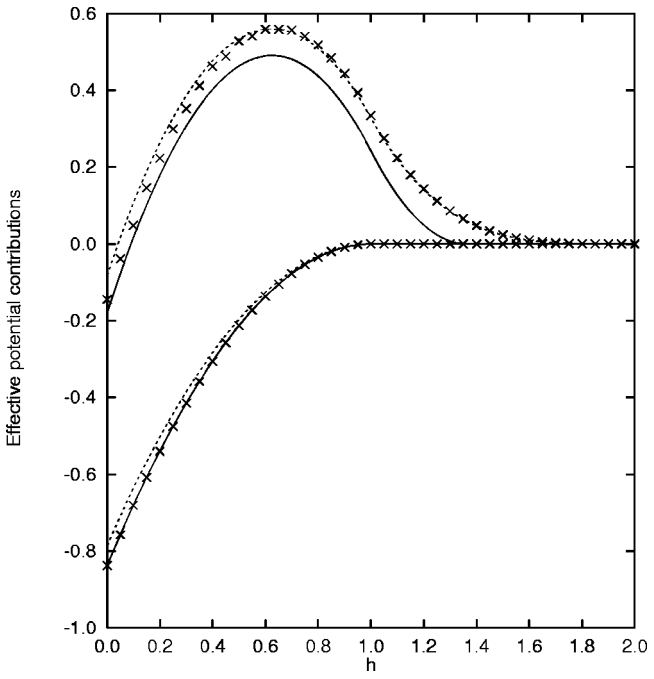

FIG. 1. Contributions to the effective potential between large particles for $R=0.10$. The distances are given in terms of h, $h=(r-\sigma_l)/\sigma_s$. The effective contributions are multiplied by the size ratio R. Such scaling produces similar curves for different values of R. Upper curves represent the terms $-RB\nu_2(r)/\sigma_s^6$. Below, the terms $-R\nu_1(r)/\sigma_s^3$ are plotted. Continuous lines show the effective contributions used in this work. Crosses represent the exact results for the two body interaction. The results from Ref. [5] are given by dashed lines.

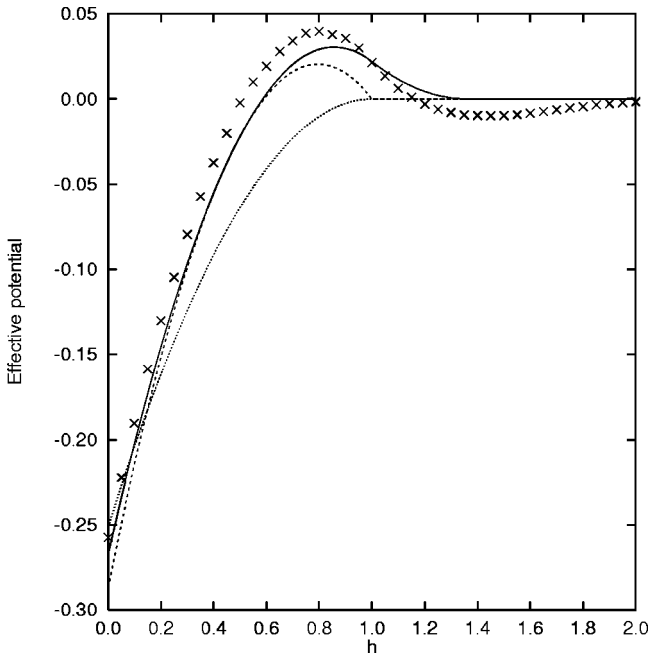

FIG. 2. Scaled effective potentials $\beta R u_{\text{effec}}(r)$ between large particles for $\rho_0\sigma_s^3=0.30$ and size ratio $R=0.10$. In the figure for such conditions we plot $R\beta u^{(2)}_{\text{effec}}\equiv -R[\rho_0\nu_1(r)+B\rho_0^2\nu_2(r)]$ (continuous line), and $R\beta U^{(1)}_{\text{effec}}\equiv -R\rho_0\nu_1(r)$ (pointed line), and the crosses represent the exact evaluation (up to third order) of the two body effective interaction which, at the current density, is expected to represent the total interaction quite well. The dashed line correspond to an effective potential (proposed in Ref. [10]), which was used in Ref. [18] in their study of the phase diagram of AHSM.

III. PHASE EQUILIBRIA

It is now well established that the range of pair interaction plays a major role in the existence of (stable) liquid-vapor phase equilibria. Thus it seems unlikely to find phase equilibria involving two phases with disorder with respect to large particles in the type of mixtures we are dealing with. Recent work has shown that short range interactions can produce the coexistence of ordered phases with the same symmetry [13]. In order to analyze these effects in our systems, we have studied by computer simulation the phase diagram in situations of low activity of the small component. Thermodynamic integration (TI) and the *so-called* Clausius-Clapeyron (or Gibbs-Duhem) integration schemes [19,20] have been used to evaluate the phase diagrams at the two levels of approach described in Sec. II.

In order to perform Clausius-Clapeyron integration, one starts from certain conditions where phase equilibrium exists and is well characterized, and proceeds to change the relevant thermodynamic variables in such a way that thermal, mechanical, and chemical equilibria between the phases are kept along the trajectory. Those ideas apply in our case as follows. In an ensemble defined by the variables $\beta\Pi$, N_l, and ρ_0, we consider two phases in equilibrium (we neglect the trivial contribution of the temperature for hard core mixtures). We have to establish a starting point on the $(\beta\Pi, \rho_0)$ plane in such a way that we have equal chemical potential of the solute in both phases. The rest of equilibrium conditions are readily fulfilled in our working ensemble. For such a state and subsequent ones one can perform $(N_l, \beta\Pi, \rho_0)$ simulations for both phases, and use the results to move along a $(\rho_0, \beta\Pi)$ trajectory that guarantees that chemical potential of large particles is kept equal in both phases.

Starting from the differential form of the Gibbs free energy G, we sketch the thermodynamics equations involved in the transformations introduced in Sec. II. Such transformations allow us to express, at the end, the problem in terms of the osmotic pressure and the density of a pure solvent system:

$$d(\beta G)=Vd\beta p+\beta\mu_l dN_l+\beta\mu_s dN_s, \tag{3.1}$$

where μ_l is the chemical potential of the solute. By a Legendre transformation, and recalling the equality $G=\Sigma_i N_i\mu_i$, we introduce the chemical potential of the solvent as a relevant variable:

$$\begin{aligned} d(\beta\mu_l N_l)&=d(\beta G-\beta\mu_s N_s)\\ &=Vd(\beta p)+\beta\mu_l dN_l-N_s d(\beta\mu_s). \end{aligned} \tag{3.2}$$

A pair of transformations allows us to use the reference solvent density ρ_0 and the osmotic pressure $\beta\Pi$ as relevant variables instead of $\beta\mu_s$ and βp:

$$d(\beta\mu_l N_l)=Vd(\beta p)+\beta\mu_l dN_l-\frac{N_s}{z_s}dz_s, \tag{3.3}$$

$$d(\beta\mu_l N_l) = V d(\beta p) + \beta\mu_l dN_l - \frac{N_s}{z_s}\frac{\partial z_s}{\partial \rho_0} d\rho_0, \tag{3.4}$$

$$d(\beta\mu_l N_l) = V d(\beta\Pi) + \beta\mu_l dN_l + \left[V\left(\frac{\partial[\beta p_0]}{\partial \rho_0}\right) - \frac{N_s}{z_s}\left(\frac{\partial z_s}{\partial \rho_0}\right)\right] d\rho_0. \tag{3.5}$$

The term between brackets can be evaluated using the partition functions developed above to produce (in the second-order approach):

$$\left(\frac{\partial[\beta N_l \mu_l]}{\partial \rho_0}\right)_{N_l,\beta\Pi} \simeq V\left(\frac{\partial[\beta p_0]}{\partial \rho_0}\right) - \frac{N_s}{z_s}\left(\frac{\partial z_s}{\partial \rho_0}\right) \simeq -\left(\frac{\partial \ln Q^{(2)}}{\partial \rho_0}\right)_{N_l,\beta\Pi}, \tag{3.6}$$

$$\left(\frac{\partial[\beta N_l \mu_l]}{\partial \rho_0}\right)_{N_l,\beta\Pi} = N_l v_l[\alpha^3 + 2\rho_0 B(2\alpha^3 - \alpha_d^3)] + U_1 + 2\rho_0 U_2, \tag{3.7}$$

where

$$U_1 = -\sum_{i<j}^{N_l} \nu_1(r_{ij}), \tag{3.8}$$

$$U_2 = -B\sum_{i<j}^{N_l} \nu_2(r_{ij}). \tag{3.9}$$

In the following we will use superindices I and II to distinguish between thermodynamical properties of two different phases. In a differential change of ρ_0 and $\beta\Pi$ we will obtain:

$$d\beta N_l(\mu_l^I - \mu_l^{II}) = (V^I - V^{II}) d(\beta\Pi) + \left[\left(\frac{\partial[\beta N_l \mu_l^I]}{\partial \rho_0}\right)_{\beta,N_l,\beta\Pi} - \left(\frac{\partial[\beta N_l \mu_l^{II}]}{\partial \rho_0}\right)_{\beta,N_l,\beta\Pi}\right] d\rho_0. \tag{3.10}$$

Therefore, the coexistence lines, which fulfill the condition $\mu_l^I = \mu_l^{II}$, can be drawn as

$$0 = \Delta V d\beta\Pi + \Delta(U_1 + 2\rho_0 U_2) d\rho_0, \tag{3.11}$$

$$\left(\frac{d\beta\Pi}{d\rho_0}\right)_{coex} = -\frac{\Delta(U_1 + 2\rho_0 U_2)}{\Delta V}, \tag{3.12}$$

where the Δ symbols express the differences of the corresponding property between both phases. The equation for the simulation using the first-order approach appears by taking $B = 0$, which makes $U_2 = 0$.

IV. SIMULATION DETAILS

Different simulation runs were performed in the ensemble described in previous sections. The number of particles was $N_l = 256$ in all cases. A second-order predictor corrector technique was used to perform Clausius-Clapeyron integration. It is probably worthless to use more sophisticated schemes because of the softness of the ρ_0-$\beta\Pi$ line, which makes the accuracy in the determination of $(d\beta\Pi/d\rho_0)$ the main source of error in the integration. The integration scheme was started from $\rho_0 = 0$. In such a case one has a pure system of large particles, and therefore the initial osmotic pressure $\beta\Pi\sigma^3 \simeq 11.71$ corresponds to the melting pressure of the HS's [21,22]. According to the previous theoretical scheme the mixture can be viewed as a pure system with particles interacting through an effective potential. In this scenario ρ_0 plays the role of the inverse of the temperature, with an effective potential that also depends on such a temperature.

In the processes of Clausius-Clapeyron integration, apparently an irreversible transition was found in the *crystal* branch. In order to overcome the problems due to either the irreversibility associated with a first-order transition in the *crystal* phase between two fcc lattices at different densities, or the presence of large fluctuations in the vicinity of a metastable critical point of the same kind, we performed TI (at different pressures in both fluid and crystal phases to locate the coexisting densities for values of ρ_0 greater than those where the instabilities were observed).

V. RESULTS

We have performed simulations to determine approximate phase diagrams using both first- and second-order expansions of Ω for $R = 0.10$ and 0.05. The phase diagrams of the systems considered in first- and second-order approaches are plotted in Figs. 3–6. The diagram corresponding to the second-order approach for $R = 0.10$ shows an isostructural crystal-crystal equilibrium which terminates at a critical point (see Fig. 4). For the same value of R in the phase diagram evaluated with the first-order effective potential, no triple point was found; however, an abrupt change of the crystal density in the phase diagram indicates either that the reference density range where such a crystal-crystal coexistence occurs is very small, or that such an equilibrium becomes metastable because it is preempted by the fluid crystal equilibrium. For the smallest size ratio ($R = 0.05$) the isostructural crystal-crystal transition appears in both orders of approach (Fig. 6). On the other hand, no fluid-fluid equilibria have been found for any of the cases analyzed in this work. The general shape of the phase diagrams (Figs. 3 and 5) seems to indicate that such equilibria, if they exist, become metastable with respect to the fluid-crystal transition. Re-

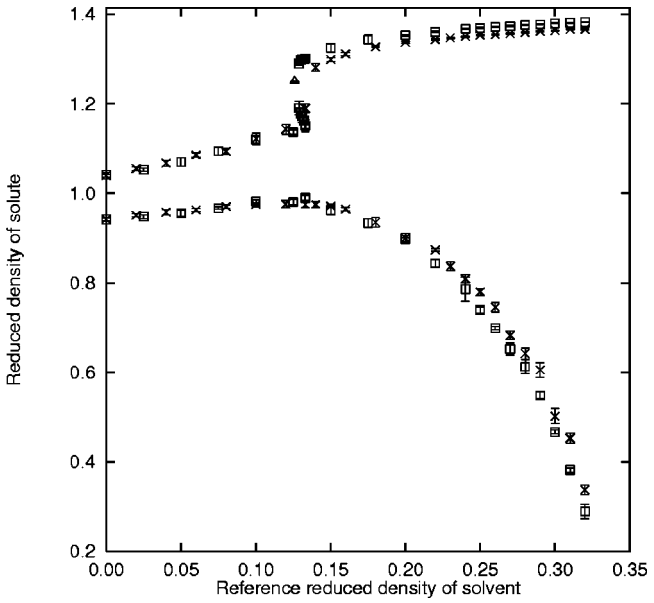

FIG. 3. Phase diagrams (binodal lines) of a hard sphere mixture with $R=0.10$ in the $(\rho_l\sigma_l^3,\rho_0\sigma_s^3)$ plane using first- (crosses) and second-order (squares) approaches to the grand potential of the solvent. Estimated error bars (2σ) are also shown.

cently, Dijkstra, van Roij, and Evans have found [18] such metastable phase transitions by performing a computer simulation with an effective potential [10], using an approach to the problem similar to the one proposed in this work. The effective potential used in Ref. [18] is slightly different to the one developed in this work (see Fig. 2 for a particular realization of the effective potentials). For low values of $\rho_0\sigma_s^3$ the attractive well of the potentials of Ref. [10] is deeper and wider than both the one developed in this work and the exact one. The slight differences in well width are, probably, the reason why no solid-solid stable equilibrium was observed in Ref. [18] for $R=0.10$.

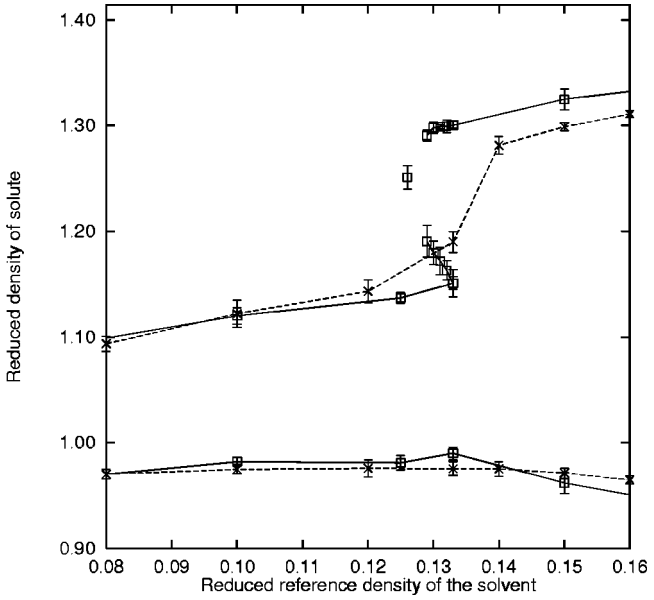

FIG. 4. Detail of the phase diagrams of a hard sphere mixture with $R=0.10$. Symbol meanings are as Fig. 3. Lines are just to join the points.

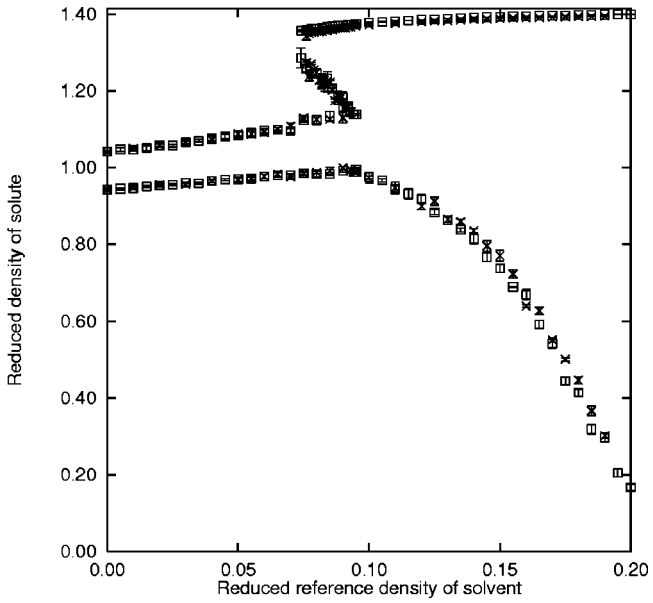

FIG. 5. Phase diagrams of a hard sphere mixture with $R=0.05$ using first- and second-order approaches to the grand potential of the solvent. See Fig 3 for symbol explanations.

On the other hand in our diagrams the fluid phase in equilibrium with a solid at low values of the solvent density shows larger densities than those in Ref. [18]. These unexpected differences might be produced by the interpolation scheme used in Ref [18] to perform TI. The rest of the diagram is quite similar, and the small differences can safely be ascribed to the different effective interactions used.

The similarities between the diagrams obtained using first- and second-order approaches to the effective potentials, and also with those in Ref. [18], leads us to think that the particulars of the depletion potential model have a small influence on the general features of the diagram, at least in the solvent densiy region studied in this work.

In order to check the quality of the approximations, we

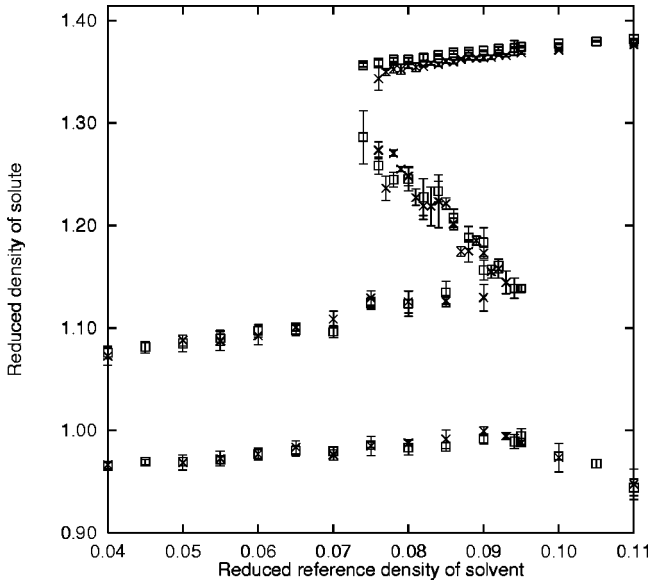

FIG. 6. Details of the phase diagrams for $R=0.05$. Symbols are as in preceding figures.

TABLE I. Comparison of the results of simulations with effective potentials with exact results for $R=0.10$. The subscripts indicate the kind of calculation, $O1$ and $O2$ refer to the simulation using first- and second-order effective potentials, respectively. The procedure to evaluate the ''exact'' values in indicated in the text.

Phase	$\rho_0\sigma_s^3$	$\beta\Pi\sigma_l^3$	$(\rho_l\sigma_l^3)_{O1}$	$(\rho_l\sigma_l^3)_{O2}$	$(\rho_l\sigma_l^3)_{\text{exact}}$	$(\rho_s\sigma_s^3)_{O1}$	$(\rho_s\sigma_s^3)_{O2}$	$(\rho_s\sigma_s^3)_{\text{exact}}$
Fluid	0.32	0.36	0.293(7)	0.258(12)	0.256	0.255(15)	0.270(15)	0.269
Crystal	0.30	24	1.3744(10)	1.3841(6)	1.3870(4)	0.0297(2)	0.0437(2)	0.0429(5)

can compare some results with ''exact'' data for two cases with $R=0.10$ for $\rho_0\sigma_s^3\simeq 0.30$. One of the cases corresponds to the fluid branch of the fluid-crystal transition. The results from computer simulation are compared with data coming from an empirical equation of state (EOS), the so-called Boublik, Mansoori, Carnahan, and Starling (BMCSL) EOS [23], which is supposed to be accurate for this case of low packing fractions of both components. On the other hand we have performed a simulation in a $N_l,\beta\mu_s,\beta p$ ensemble corresponding to the situation of $\rho_0\sigma_s^3=0.30$ and $\beta\Pi\sigma_l^3=24$. The relation between ρ_0 and $\beta\mu_s$ and βp_0 can also be extracted from the BMCSL EOS.

In Table I we collect these data, and it can be observed how the second-order approach compares quite well with the ''exact'' results. This agreement leads us to point out that the second-order approach seems to be accurate enough to determine the phase diagram, at least up to the values of ρ_0 used in this work.

VI. CONCLUSIONS

The results presented in this work seem to show that there is not a stable *fluid-fluid* phase equilibria in very asymmetric mixtures of hard spheres. Even if the work is centered on situations where the packing fraction of the small component is rather low, it is to be expected that the behavior will remain similar to that shown in these results.

It has also been observed that the shape of the phase diagrams evaluated using first- and second-order approaches is quite similar in the $\beta\Pi,\rho_0$ plane. Moreover the diagrams are quite similar to those reported in Ref. [18], when a similar approach was used, but with different effective potentials. Finally, the presence of isostructural solid-solid phase equilibria in these systems seem to indicate the possibility of finding this phenomenology in *real* systems formed by colloidal mixtures.

ACKNOWLEDGMENTS

The authors acknowledge the financial support of DGICYT/Spain (Grant No. PN95-072-C03-02). We thank J.A. Cuesta and C. Vega for stimulating discussions, and M. Dijkstra, R. van Roij, and R. Evans for providing us with a copy of their unpublished work.

[1] C. Caccamo, Phys. Rep. **274**, 1 (1996), and references therein.

[2] (a) A. Z. Panagiotopoulos, in *Observation, Prediction and Simulation of Phase Transitions in Complex Fluids*, Vol. 460 of *NATO Advanced Study Institute Series C: Mathematical and Physical Sciences*, edited by M. Baus, L. F. Rull, and J. P. Ryckaert (Kluwer, Dordrecht, 1995), p. 463; (b) B. Smit, in *Computer Simulation in Chemical Physics*, Vol. 397 of *NATO Advanced Study Institute Series C: Mathematical and Physical Sciences*, edited by M. P. Allen and D. J. Tildesley (Kluwer, Dordrecht, 1993), p. 173.

[3] S. Akasura and F. Oosawa, J. Chem. Phys. **22**, 1255 (1954).

[4] A. Vrij, Pure Appl. Chem. **48**, 471 (1976).

[5] Y. Mao, M. E. Cates, and H. N. W. Lekkerkerker, Physica A **222**, 10 (1995).

[6] T. Biben, P. Bladon, and D. Frenkel, J. Phys.: Condens. Matter **8**, 10 799 (1996).

[7] P. Attard, J. Chem. Phys. **91**, 3083 (1989).

[8] P. Attard and G. N. Patey, J. Chem. Phys. **92**, 4970 (1990).

[9] R. Dickman, P. Attard, and V. Simonian, J. Chem. Phys. **107**, 295 (1997).

[10] B. Götzelmann, R. Evans, and S. Dietrich, Phys. Rev. E **57**, 6785 (1998).

[11] E. Lomba and N. G. Almarza, J. Chem. Phys. **100**, 8367 (1994).

[12] M. H. J. Hagen and D. Frenkel, J. Chem. Phys. **101**, 4093 (1994).

[13] P. Bolhuis, M. Hagen, and D. Frenkel, Phys. Rev. E **50**, 4880 (1994).

[14] N. G. Almarza and E. Enciso, *Proceedings of the VII Spanish Meeting on Statistical Physics FISES'97, Anales de Física, Monografías RSEF* (Ciemat, Madrid, 1998), Vol. 4, p. 159.

[15] M. P. Allen and D. J. Tildesley, *Computer Simulation of Liquids* (Clarendon, Oxford, 1987).

[16] J. P. Hansen and I. R. McDonald, *Theory of Simple Fluids* (North-Holland, Amsterdam, 1985).

[17] Considering a diagrammatic expansion of the three-body contributions to the potential of the mean force, and taking into account the configurations of three large particles (without overlaps between them) and two small overlapping particles, $R_2^{(2)}$ corresponds to the lowest size ratio R for which three-dimensional configurations can be built, in which every large particle overlaps with (at least) one small particle and each small particle overlaps with (at least) one large particle. To determine $R_2^{(2)}$, one can consider an equilateral triangle of side

length σ_l; on each vertex a sphere of radious $\sigma_l(1+R)/2$ can be located. For $R \leqslant 2/\sqrt{3}-1 \equiv R_2$ no triple overlap occurs. It is also possible to evaluate the minimum distance between one of the spheres and the overlapping volume of the other two; for $R=R_2^{(2)}$, such a distance is equal to $\sigma_l R$.

[18] M. Dijkstra, R. van Roij, and R. Evans, Phys. Rev. Lett. **81**, 2268 (1998).

[19] D. A. Kofke, Mol. Phys. **78**, 1331 (1993).

[20] D. Frenkel, in *Observation, Prediction and Simulation of Phase Transitions in Complex Fluids* [Ref. [2(a)]], p. 357.

[21] W. G. Hoover and F. H. Ree, J. Chem. Phys. **49**, 3609 (1968).

[22] W. G. T. Kranendonk and D. Frenkel, Mol. Phys. **72**, 679 (1991).

[23] T. Boublik, J. Chem. Phys. **53**, 471 (1970); G. A. Mansoori, N. F. Carnahan, K. E. Starling, and T. W. Leland, *ibid.* **54**, 1523 (1971).